Available online at www.sciencedirect.com
SCIENCE DIRECT®
ELSEVIER
Journal of Power Sources 156 (2006) 755–762
JOURNAL OF POWER SOURCES
www.elsevier.com/locate/jpowsour

An ultracapacitor circuit for reducing sulfation in lead acid batteries for Mild Hybrid Electric Vehicles

Adam W. Stienecker[a,*], Thomas Stuart[a], Cyrus Ashtiani[b]

[a] The University of Toledo, Electrical Engineering and Computer Science Department, 2801 West Bancroft St., Mail Stop #308, Toledo, OH 43606, USA
[b] DaimlerChrysler, AG, Auburn Hills, MI, USA

Received 9 May 2005; received in revised form 7 June 2005; accepted 7 June 2005
Available online 15 August 2005

Abstract

The nickel metal hydride (NiMH) batteries used in most hybrid electric vehicles (HEVs) provide satisfactory performance, but are quite expensive. In spite of their lower energy density, lead acid batteries would be much more economical except they are prone to sulfation in HEV applications. However, sulfation can be greatly reduced by a circuit that uses an ultracapacitor in conjunction with the battery. The resulting system will provide much cheaper energy storage if ultracapacitor prices can be reduced to levels predicted by some manufacturers.

Keywords: Valve regulated lead acid battery (VRLA); Ultracapacitor; Sulfation; High rate partial state of charge; Hybrid electric vehicle (HEV)

1. Introduction

Mild Hybrid Electric Vehicles (HEVs) are generally defined to be those that use their batteries only to provide energy boost or storage for short periods such as acceleration, engine start-up, idle-stop, and regenerative braking (regen). As a result, these batteries experience very high and frequent surge currents, and they must withstand thousands of deep charge/discharge cycles.

One of the more serious problems with these vehicles is the present dependence on very expensive batteries such as nickel metal hydride (NiMH) or lithium ion (LiIon). The present battery of choice, NiMH, provides a much higher energy density than lower cost lead acids, but perhaps even more important is its higher reliability. From a performance standpoint, LiIon appears to be superior to either NiMH or lead acid, but high cost and safety concerns have limited its use. At present, lead acid actually is the only economically attractive battery, but it is ill-suited for HEVs because of the frequent deep cycling and the fact that the state of charge (SOC) must be held below about 80% to accept regen energy. The basic problem is that these conditions lead to a process called sulfation on the negative battery plate which causes early failure [1–6].

Another device, called an ultracapacitor (UC), has been proposed to reduce some of the problems with HEV batteries, especially cold weather performance. UCs themselves also are presently very expensive, but this is primarily due to their early state of development and low production volumes. Unlike NiMH batteries, UCs contain no expensive alloys, and their projected cost in high production is favorable. Because their operation does not employ a chemical reaction, they are much more robust than batteries, and their lifetime is expected to exceed that of an HEV.

The easiest way to supplement a battery with a UC is to simply connect the two in parallel as shown in Fig. 1 for a 36 V mild parallel hybrid system. Because the UC has a much higher power density than the battery, surge current capacity is now much higher, especially at low temperatures. However, the battery has a much higher energy density than the UC, so the optimum system includes both devices.

* Corresponding author. Present address: Ohio Northern University, Department of Technological Studies, Ta&t Memorial Room 208, Ada, OH 45810, USA. Tel.: +1 419 772 2171; fax: +1 419 772 2688.
E-mail address: adam@ieee.org (A.W. Stienecker).

0378-7753/$ – see front matter © 2005 Elsevier B.V. All rights reserved.
doi:10.1016/j.jpowsour.2005.06.014

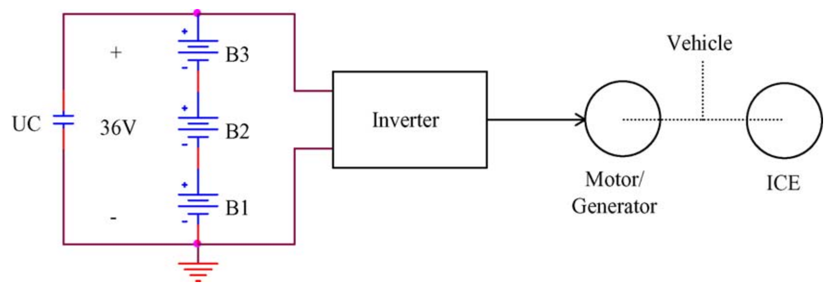

Fig. 1. Parallel battery/ultracapacitor system.

Unfortunately, a simple parallel connection may do little to reduce the sulfation problem for a lead acid. The UC will reduce the surge currents in the battery somewhat, but the battery is still exposed to these currents, and its SOC still must be held somewhere below 80% to accept regen.

However, most of the inverters used to drive the electric traction motor in an HEV have a fortuitous characteristic that allows the circuit in Fig. 2 to address the sulfation problem, i.e., the inverter can operate over a 2:1 input voltage range. In the system in Fig. 2, the UC nominally operates at about 36 V, but this voltage can vary from 45 V to the nominal battery voltage of 24 V. During regen, the diode, D, blocks the regen current so the UC will absorb all of the regen energy as V_{UC} increases. In the boost mode, UC will supply all of the boost current until V_{UC} discharges to V_B. At $V_{UC} = V_B$, D conducts and the remaining boost current is supplied by the battery. S2 and R are only used to prepare for charging the battery while the HEV is parked, as will be explained later.

Thus the basic function on the circuit in Fig. 2 can be summarized as follows:

1. The UC absorbs all of the regen current.
2. The UC also provides all of the boost current until $V_{UC} = V_B$ and D conducts, i.e., the battery is used only to help supply the final stage of higher energy boost currents, and the UC supplies all of the lower energy boost currents.
3. Since it absorbs no regen energy, there is no need to keep the battery SOC below 100%, and when the proper conditions are met, the traction motor can be operated as a generator to quickly recharge the battery close to 100%.

The necessary conditions for recharging the battery are:

1. The switch, S1, is closed.
2. The internal combustion engine (ICE) is running so it can drive the generator.
3. Neither boost nor regen is present.
4. $V_{UC} = V_B$ (or at least within about ±10%).

Condition 3 is imposed to protect S1, which is sized only to carry the battery charging current, which is much smaller than the peak boost and regen currents. Boost and regen can always be initiated during a charging session, but S1 is first opened. Likewise condition 4 is necessary to prevent the high surge current through S that could occur if S is closed when $V_{UC} > V_B$. If the vehicle is in motion, V_{UC} can be reduced to V_B simply by providing a boost current. When the vehicle is parked, the resistor, R, can be used to reduce V_{UC}, but it is obviously more efficient to avoid this mode.

Although most of the energy from the 42 V system will be used for traction, some applications also may require it to supply other loads as well. If so, these loads will probably operate at some lower voltage, e.g. 12 V. More than one method can be used to derive these lower voltages, one possibility being shown in Fig. 3. In this arrangement, the 12 V bus is connected to B1, and B1 is regulated using a relatively small and simple switching regulator. Since it supplies the 12 V bus, B1 will discharge faster than B2, but the switching regulator provides extra charge to B1 to maintain equalization with B2. Since B1 supplies more energy, the lifetimes of B1 and B2 will have better parity if B1 has a larger capacity than B2. The circuit in Fig. 3 also can be turned off to avoid discharging UC when idle-stop operation of the ICE is employed. It is also noted that R and S2 in Fig. 2 are no longer required since the regulator can be used to reduce

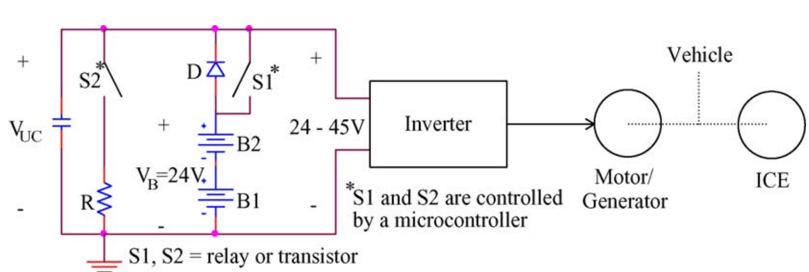

Fig. 2. Variable voltage battery/ultracapacitor system with blocking diode and bypass switch [7].

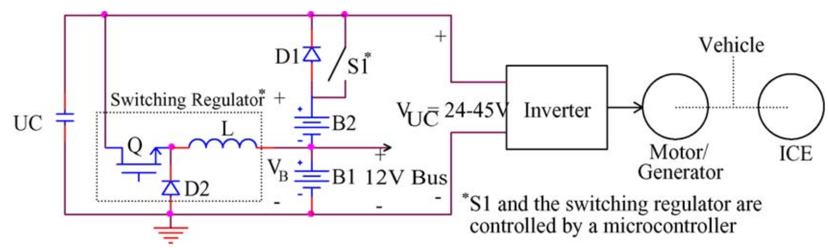

Fig. 3. Variable voltage system with a regulated 12 V bus.

V_{UC} to V_B before charging the battery while the HEV is parked.

2. Ultracapacitors

Due to recent advances in technology [8–12], manufacturers are now able to produce capacitors in the 2700+ F range at a cell voltage of about 2.5 V. However, present values of only 5–10 Wh kg^{-1} [10] indicate the energy density of a UC is much lower than the 28+ Wh kg^{-1} [9] available in a lead acid.

On the basis of energy density alone, the battery is clearly the better choice, but when power density is also considered, the ultracapacitor becomes more attractive. The main reason for the large difference in power density between the battery and the UC is the method used to store energy. In a battery, energy is stored through a chemical reaction, which is initiated during charging and reversed during discharge. This chemical reaction is equivalent to an additional source impedance which limits power density. UCs, on the other hand, store energy in a completely different manner, i.e., charge separation [9]. This allows the energy to be stored and released without any chemical reaction taking place, and the UC can accept and release energy very fast and with low losses, i.e., it has a higher power density. UCs have been produced with a maximum power density above 5 kW kg^{-1}, as compared to a lead acid with a power density of about 0.5 kW kg^{-1}, for a matched impedance discharge [9].

The availability of UCs over the last 3–4 years has steadily improved, and several companies now have UCs available that appear to be acceptable for HEVs [13–18]. Due to current low levels of production, the prices for UCs are still very high. However, manufacturers claim these prices are largely due to economies of scale, and they are expected to drop drastically as production levels increase.

3. HEV batteries

There have been several advances in battery technology due to the market for electric and hybrid electric vehicles. Lead acids have, of course, been the predominant automotive battery, but in more advanced types such as NiMH and LiIon are now available. These batteries indeed have certain advantages over the lead acid, but they also have two large disadvantages: cost and complexity.

The lead acid battery is, by far, the cheapest and simplest battery technology currently on the market, but they also have lower energy density and longevity [19]. Their main competitors, NiMH and LiIon, both have much higher energy densities with the LiIon possessing the highest of the three. NiMH also has a high self-discharge rate and it is difficult to accurately measure its state of charge (SOC) [19]. LiIon is more complicated to charge than the other two due to safety hazards inherent in the battery [19] and this added complexity also adds to its already high cost.

4. The Hybrid Energy Storage System (HESS)

The term HESS simply means an energy storage system containing both a battery and an ultracapacitor. The concept is generally successful because it exploits the strengths and compensates for the weaknesses of each storage device. When these systems are used, the batteries can be designed for higher energy density at the expense of lower power density. Conversely, the UC can be designed for higher power density at the expense of lower energy density. Previous studies [20–26], most of which were based on a simple parallel combination as in Figs. 1 and 4, have shown that an ultracapacitor–battery combination does indeed increase the performance.

Because of its lower resistance, the UC is able to shield the battery from at least a portion of the current pulses and thus extend the battery lifetime somewhat [20]. However, the battery is still exposed to most of the pulse, so the improvement in lifetime will not be as great as desired. This lifetime

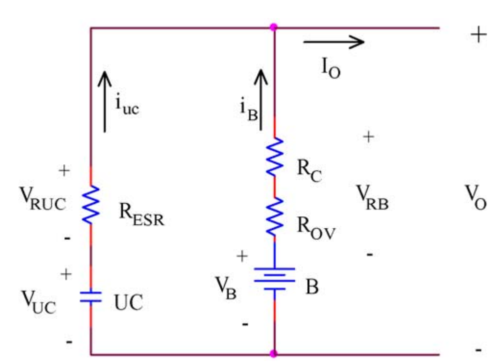

Fig. 4. Equivalent circuit of a parallel battery/ultracapacitor.

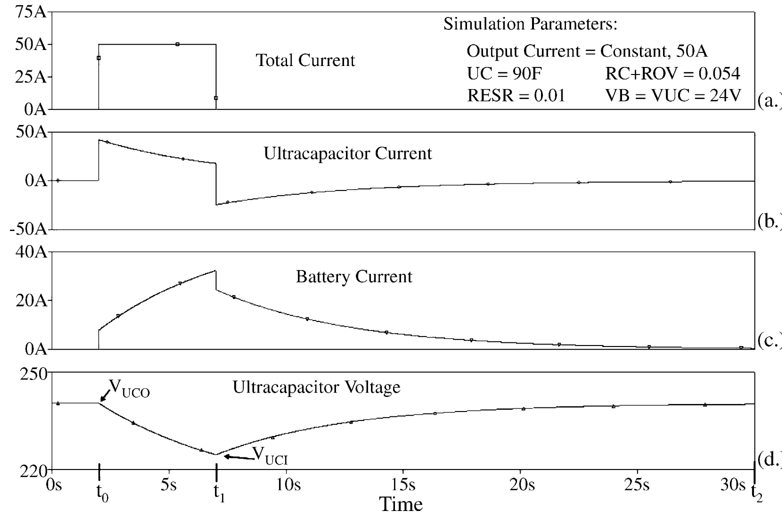

Fig. 5. Hybrid ultracapacitor–battery simulated discharge current waveforms.

extension is due to reducing the ionization within the battery, a phenomenon that is not present in the UC.

If the parameters in Fig. 4 can be determined, the circuit equations can be used to predict the behavior for various types of loads. Fig. 5 shows the results of a simulation where the constant current pulse in Fig. 5(a) is applied to the circuit in Fig. 4.

From t_0 to t_1 the UC current in Fig. 5(b) supplies most of the energy while the battery current in Fig. 5(c) ramps up slowly. Between t_1 and t_2 the battery is actually recharging the UC. This is due to the difference between the equivalent series resistance of the UC, R_{ESR}, and the combination of the over voltage resistance (R_{ov}) and the Coulomb resistance (R_{c}) in the battery [27]. R_{ov} in Fig. 4 is not an actual resistance in the usual sense but a term that represents the energy losses required to charge or discharge the battery. This simulation used a constant value for R_{ov}, but this term actually is very non-linear [27] with respect to the current and the state of charge. In Fig. 4 we see that between t_0 and t_1, $V_{\mathrm{RUC}} + V_{\mathrm{UC}} = V_{\mathrm{RB}} + V_{\mathrm{B}}$, but $V_{\mathrm{RUC}} \neq V_{\mathrm{RB}}$, and $V_{\mathrm{B}} \neq V_{\mathrm{UC}}$. Therefore, at time t_1, where the applied current load drops to 0, current will flow from UC to B since $V_{\mathrm{UC}} > V_{\mathrm{B}}$.

If we assume that the battery voltage (V_{B}), the output voltage (V_{O}), the resistances, and the capacitances are all constant then a closed form solution can be obtained.

A mathematical analysis gives the following for $0 \leq t \leq t_1$:

$$i_{\mathrm{UC}}(t) = \frac{(V_{\mathrm{UC}_0} - V_{\mathrm{B}}) + I_{\mathrm{O}} R_{\mathrm{B}}}{R_{\mathrm{B}} + R_{\mathrm{ESR}}}\, \mathrm{e}^{-t/\tau} \quad (1)$$

where V_{UC_0}, the initial ultracapacitor voltage; $R_{\mathrm{B}} = R_{\mathrm{C}} + R_{\mathrm{OV}}$; $\tau = C(R_{\mathrm{B}} + R_{\mathrm{ESR}})$; C, capacitance of the ultracapacitor; V_{O}, output voltage, constant; V_{B}, battery voltage, constant and

$$i_{\mathrm{B}}(t) = I_{\mathrm{O}} - i_{\mathrm{UC}}(t) \quad (2)$$

where I_{O}, output current, constant; i_{UC} (t), ultracapacitor current; i_{B} (t), battery current.

From t_0 to t_1, assuming that the ultracapacitor has been fully charged to the voltage of the battery, i_{UC} becomes:

$$i_{\mathrm{UC}}(t) = \frac{I_{\mathrm{O}} R_{\mathrm{B}}}{R_{\mathrm{B}} + R_{\mathrm{ESR}}}\, \mathrm{e}^{-t/\tau}. \quad (3)$$

From t_1 to t_2, i_{UC} becomes:

$$i_{\mathrm{UC}}(t) = \frac{V_{\mathrm{UC}_1} - V_{\mathrm{B}}}{R_{\mathrm{B}} + R_{\mathrm{ESR}}}\, \mathrm{e}^{-t/\tau}. \quad (4)$$

where $V_{\mathrm{UC}_1} = I_{\mathrm{O}} R_{\mathrm{B}}(\mathrm{e}^{-T_{\mathrm{p}}/\tau} - 1) + V_{\mathrm{UC}_0}$ (the UC voltage at time t_1) (see Fig. 5(d)); $T_{\mathrm{p}} = t_1 - t_0$, current pulse length in seconds.

In Fig. 5(d) notice the UC voltage before the pulse, V_{UC_0}, and the UC voltage immediately following the pulse, V_{UC_1}. Immediately after the pulse the UC voltage begins to rise because the battery is recharging the UC. It continues to rise until $V_{\mathrm{UC}} = V_{\mathrm{B}}$. Naturally, the UC current also reverses direction at t_1 when the UC begins to charge.

5. The proposed Ultracapacitor–Battery Energy Storage System

As previously noted the conventional HESS in Fig. 1 offers many advantages, but there is room for improvement. The conventional system provides the battery with a limited shield from the large power surges during a typical driving cycle, but the battery still sees most of each current pulse. Unfortunately, the conventional system also does not address the sulfation issue in lead acid batteries.

The benefit of the UC can be increased by using multiple voltage levels within the HESS, but this is cost prohibitive if expensive DC/DC converters [28] are used. However, the alternative circuit shown in Fig. 2 avoids the limitations of the conventional system, and the additional hardware is relatively inexpensive.

In Fig. 2, UC will shield B from all boost pulses as long as V_{UC} is kept above V_B. The switch, S1, in these circuits is used only to bypass D when the batteries need to be recharged. UC must absorb all of the regen pulses since current in this direction is blocked by D, and UC also supplies all of the boost pulses until V_{UC} decreases to V_B. The variable V_{UC} is feasible since most HEV inverters can operate over a 2:1 input voltage range. For instance, in a 42 V system the inverter might function properly with an input voltage ranging from 24 V up to 48 V. If the pulse length, T_P, is greater than a certain value, T_{PC}, the battery will begin to supply most of the current and the system equations become the same as those for Fig. 1, assuming a constant voltage drop across the diode, V_D. For $0 < t < T_{PC}$, the equations for the circuit in Fig. 2 are as follows:

$$i_{UC}(t) = C\frac{\mathrm{d}v_{UC}(t)}{\mathrm{d}t} \tag{5a}$$

$$v_{UC}(t) = v_{UC_0} - \frac{1}{C}\int_0^t i_{UC}(t)\,\mathrm{d}t \tag{5b}$$

If the load is approximated by a constant power pulse, P_O:

$$P_O = v_O(t)i_{UC}(t) = \text{constant} \tag{6}$$

Substituting (5b) and $v_O(t) = v_{UC}(t) - i_{UC}(t)R_{ESR}$ into equation (6)

$$P_O = i_{UC}(t)\left(v_{UC_0} - \int_0^t i_{UC}(t)\,\mathrm{d}t\right) - i_{UC}^2(t)R_{ESR}.$$

Dividing through by $i_{UC}(t)$ and differentiating both sides yields:

$$-\frac{P_O}{i_{UC}^2(t)}\frac{\mathrm{d}i_{UC}(t)}{\mathrm{d}t} = -\frac{i_{UC}(t)}{C} - R_{ESR}\frac{\mathrm{d}i_{UC}(t)}{\mathrm{d}t}$$

and combining terms gives:

$$\frac{\mathrm{d}i_{UC}(t)}{\mathrm{d}t} + \frac{i_{UC}^3(t)}{C(i_{UC}^2(t)R_{ESR} - P_O)} = 0 \tag{7}$$

Since equation (7) does not lend itself to a closed form solution, an iterative solution is required. From equation (5a) we obtain $\mathrm{d}v_{UC}(t) = \frac{1}{C}i_{UC}(t)\,\mathrm{d}t$.

If we let $\mathrm{d}t = \Delta t$ and k = the iteration number, $\Delta v_{UC}(t) = v_{UC(k-1)} - v_{UC(k)}$, then

$$v_{UC(k)} = v_{UC(k-1)} - \frac{1}{C}i_{UC(k)}\Delta t. \tag{8}$$

From equation (6) and since $v_O = v_{UC}(t) - i_{UC}(t)R_{ESR}$,

$$P_O = v_O i_{UC}(t) = (v_{UC}(t) - i_{UC}(t)R_{ESR})i_{UC}(t).$$

Multiplying through and reconfiguring terms gives $R_{ESR}i_{UC(k)}^2 - v_{UC(k)}i_{UC(k)} + P_O = 0$

Substituting equation (8) yields $\left(R_{ESR} + \frac{\Delta t}{C}\right)i_{UC(k)}^2 - v_{UC(k-1)}i_{UC(k)} + P_O = 0$ and solving the quadratic produces:

$$i_{UC(k)} = \frac{v_{UC(k-1)} - \sqrt{v_{UC(k-1)}^2 - 4\left(R_{ESR} + \frac{\Delta t}{C}\right)P_O}}{2\left(R_{ESR} + \frac{\Delta t}{C}\right)}. \tag{9}$$

Equations (8) and (9) can now be used to perform a simulation of the circuit.

The results of one simulation using the above equations is shown in Fig. 6 for a constant pulse P_O = 10 kW for 9 s. Note that the battery does not supply current until time T_{PC} and that the UC still supplies most of the total energy. This pulse is used to simulate an acceleration boost for the vehicle.

As compared to using a battery alone, the proposed UC + B combination does not translate into meaningful fuel savings because the same amount of energy is still being supplied, but it does translate into an increase in battery lifetime. Since the UC has a rated lifetime greater than that of a typical

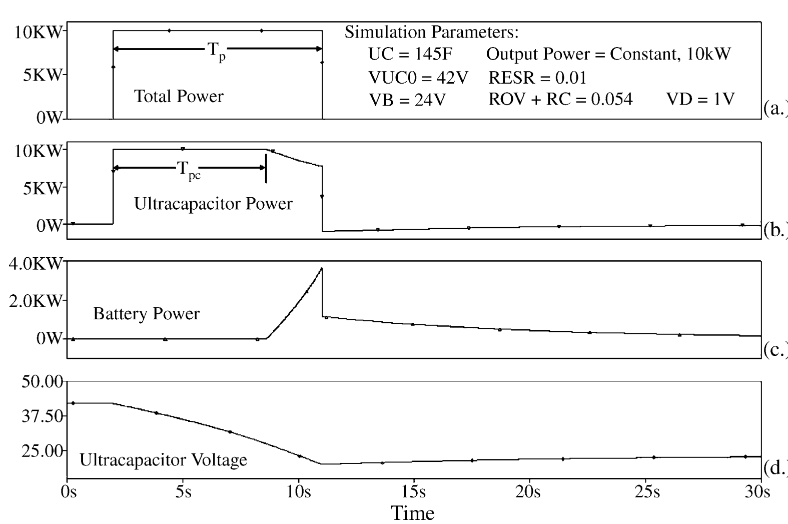

Fig. 6. Simulated constant power pulse.

vehicle, e.g., 10 years or more [29], the lifetime of the ESS is essentially limited only by the battery, which is dependant upon its use. An improvement is now achieved because the number and size of the current pulses delivered by the battery are reduced, and its SOC can be held close to 100%. This provides important advantages in reducing sulfation in a lead acid battery.

Another important aspect is the required size of the batteries since a conventional system needs a higher battery voltage and amp hour capacity than the proposed system. A typical example might be to use three series connected 12 V, 40 Ah automotive batteries. This results in a 36 V (nominal) system. The proposed variable voltage system could utilize a 36 V UC along with two 12 V 15 Ah batteries. A typical UC is fairly similar in size and weight to one 12 V, 40 Ah battery, so the total size and weight is about the same.

6. Bypass switch

The diode bypass switch can be implemented with either a mechanical or a solid state switch as shown in Fig. 7. Providing a current path in parallel with the diode is simple, but it must be used properly. The first issue is that before closing the switch, the UC must be at the same voltage level as the battery. To minimize cost, the bypass switch also should be designed to carry only the battery charge current, which is much lower than the boost and regen surge currents. While the battery is charging, the switch can be opened very quickly before initiating a boost or regen.

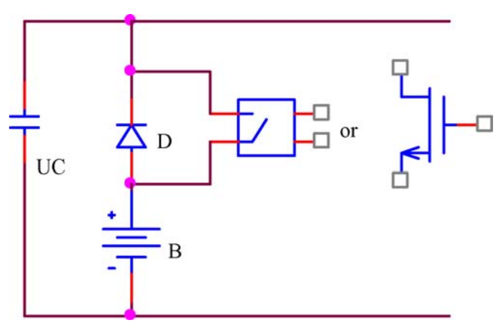

Fig. 7. Alternative bypass switches.

7. Test results

An implementation of the circuit in Fig. 2 was constructed and a series of tests were performed on the system. The UC used in this test was a NESSCAP EMHSP-0094C0-045R0 module which is rated at 94 F, 45 V. The battery pack consisted of (2) 50 Ah (c_{20}) Exide 34DC-48 12 V valve regulated lead acid (VRLA) batteries. The diode was an International Rectifier 1N4049, and the switch was a TYCO, VF7-41H11, automotive relay. The control system was implemented using a Phytec single board computer using an Infineon C505C microcontroller. All tests were performed using an Aerovironment ABC-150 Power Processing System to generate the required current pulses. The test currents were measured using two LEM LF-505S Current Transducers.

Fig. 8 shows the results of for a series of 300 A/5 s boost and regen pulses. For this pulse width the UC is large enough to both deliver and store 100% of the energy, and the battery remains inactive. Note that the regen current is not quite constant for the entire 5 s, i.e., the amplitude begins to drop before the end of the pulse. This is because the ABC-150 maximum voltage is limited to 45 V to protect the UC, and 45 V is reached before the end of the pulse. Similar protection would be provided on an HEV.

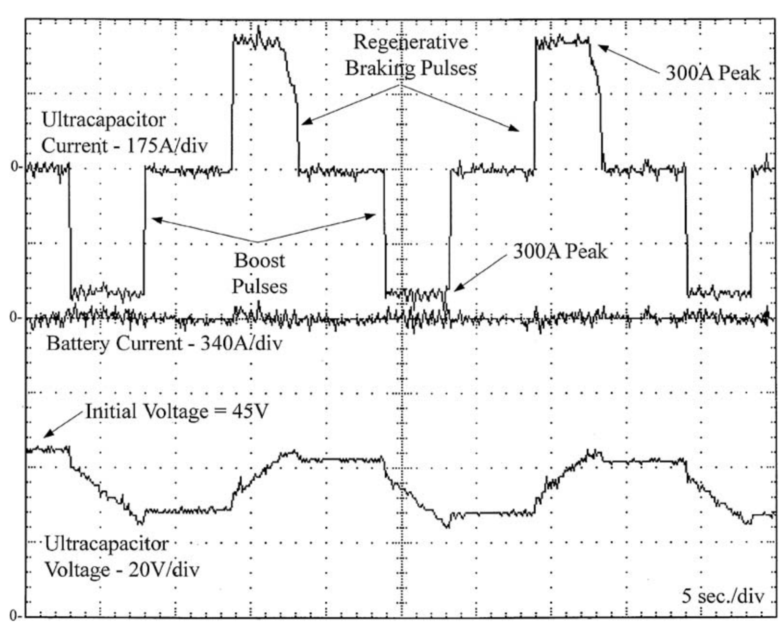

Fig. 8. Results for 300 A/5 s test currents.

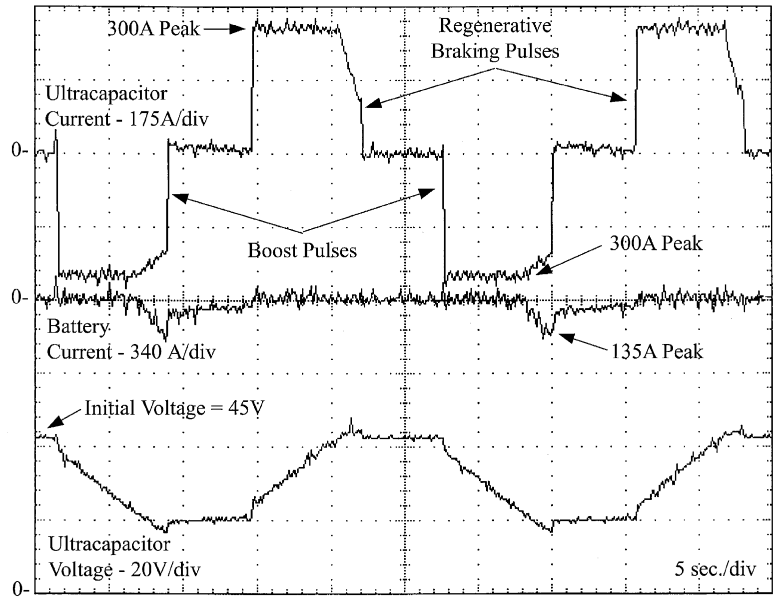

Fig. 9. Results for 300 A/8 s test currents.

If we lengthen the pulses to 8 s as in Fig. 9 the battery begins to deliver energy during the final portion of the boost pulse. As the pulse width increases, the battery supplies more of the boost energy, but it will never consume any regen energy due to the blocking diode. Each regen pulse starts to decrease before the end of the pulse, as discussed previously for Fig. 8.

For idle-stop operation where the ICE is turned off, the ESS must provide energy to run the auxiliary loads and then re-start the engine. Because of the constant idle-stop power specification, these tests where performed using constant power pulses as an alternative to the constant current pulses in Figs. 8 and 9. The test results in Fig. 10 show a 1.5 kW, 30 s load during idle-stop, followed by a constant start up pulse of 5.2 kW, 6 s. After the ICE has reached an efficient operating speed, the generator is used to recharge the UC and the test is completed by using regen energy to bring the UC back up to 100% SOC. This is represented by the 2 kW, 25 s recharge pulse and the 5 kW, 6 s regen pulse, respectively.

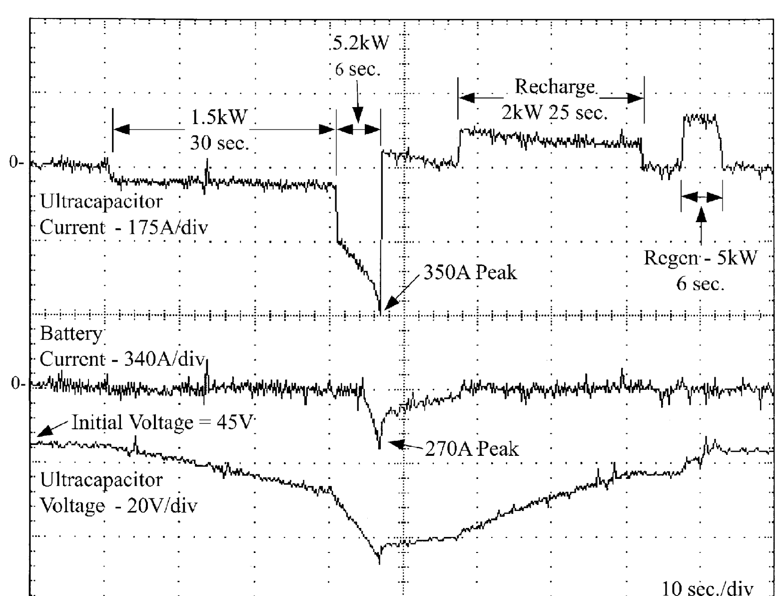

Fig. 10. Results for the idle-stop test.

8. Summary

A simple system has been presented to reduce the sulfation problem for lead acid batteries in mild HEV applications. The basic strategy is to use an ultracapacitor to process all of the regen pulses and most of the boost pulses. However, since the battery has a much higher energy density than the ultracapacitor, it is still used to advantage to complete the longer boost pulses. Since the battery sees no regen in this variable voltage system, its SOC can be held close to 100% to further reduce sulfation.

While the HEV is in motion, virtually all of the energy stored in the ultracapacitor is used only to power the HEV. There is no energy transfer between the ultracapacitor and the battery, except after a very high energy boost pulse that has discharged the ultracapacitor to the battery voltage. Some energy is then eventually transferred from the ultracapacitor to the battery, but the amount is insignificant.

At present, all components in this system except the ultracapacitor are relatively inexpensive. Future commercial applications undoubtedly will depend on the availability of lower cost ultracapacitors.

An experimental system including the necessary control equipment was built and evaluated for its technical feasibility. The system was then tested extensively with an ABC-150 HEV load simulator and was found to operate satisfactorily. Plans are now in progress to install a system of this type on-board an HEV to evaluate its performance on an actual vehicle.

Acknowledgement

This research was supported in part by NASA Grant NAG3-2790 under subcontract from Bowling Green State University and in part by a research grant from Daimler-Chrysler, AG.

References

[1] L.T. Lam, N.P. Haigh, C.G. Phyland, A.J. Urban, J. Power Sources 133 (2004) 126–134.
[2] A. Cooper, J. Power Sources 133 (2004) 116–125.
[3] G.J. May, J. Power Sources 133 (2004) 110–115.
[4] P.T. Moseley, J. Power Sources 127 (2004) 27–32.
[5] P. Ruetschi, J. Power Sources 127 (2004) 33–44.
[6] J.H. Yan, W.S. Li, Q.Y. Zhan, J. Power Sources 133 (2004) 135–140.
[7] C. Ashtiani, T. Stuart, An Energy Storage System Using an Ultracapacitor with a Switched Battery, U.S. Provisional Patent Application Serial No. 60/626,560, November 10, 2004.
[8] J. Miller, P. McClear, M. Cohen, Ultracapacitors as Energy Buffers in a Multiple Zone Electrical Distribution System, Maxwell Technologies Inc., White Paper, www.maxwell.com.
[9] A. Burke, J. Power Sources 91 (2000) 37–50.
[10] J. Mierlo, P. Bossche, G. Maggetto, J. Power Sources 128 (2003) 76–89.
[11] R. Dougal, L. Gao, S. Liu, J. Power Sources 126 (2003) 250–257.
[12] A. Chu, P. Braatz, J. Power Sources 112 (2002) 236–246.
[13] EPCOS, www.epcos.com.
[14] ESMA, www.esma-cap.com.
[15] Tavrima, www.tavrima.com.
[16] NESSCAP, www.nesscap.com.
[17] Maxwell Technologies, www.maxwell.com.
[18] PowerSystems, www.powersystems.co.
[19] D. Rand, R. Woods, R. Dell, Batteries for Electric Vehicles, Research Studies Press Ltd., Taunton, England, 1998.
[20] R. Dougal, S. Liu, R. White, IEEE Trans. Components Packag. Tech. 25 (1 (March)) (2002).
[21] F. Gagleardi, M. Pagano, G. Maestri, M. Martone, A. Tarantino, Proceedings of the 2002 IEEE International Symposium on Industrial Electronics, vol. 1, 2002, pp. 93–98.
[22] A. Trippe, A. Burke, E. Blank, Proceedings of the ESD Environmental Vehicles Conference and Exp., Dearborn, Michigan, 1995.
[23] R. Schupbach, J. Balda, M. Zolot, B. Kramer, IEEE 2003 Power Electronics Specialists Conference (PESC), Acapulco, Mexico, June 16th, 2003.
[24] J. Miller, S. Butler, SAE J. (2001).
[25] C. Holland, J. Weidner, R. Dougal, R. White, J. Power Sources 109 (2002) 32–37.
[26] X. Yan, D. Patterson, Renewable Energy 22 (2000) 177–183.
[27] A. Hande, AC Battery Heating for Cold Climates, Ph.D. Dissertation, The University of Toledo, 2002.
[28] J. Dixon, M. Ortuzar, IEEE AESS Systems Magazine, August 2002.
[29] Electric Double Layer Capacitor: BOOSTCAP Module Datasheet, Maxwell Technologies, www.maxwell.com.